SSC20-VI-10

Cathode & Electromagnet Qualification Status and Power Processing Unit Development Update for the Ascendant Sub-kW Transcelestial Electric Propulsion System

Ryan W. Conversano, Ansel Barchowsky, Vatché Vorperian, Vernon H. Chaplin, Giulia Becatti, Gregory A. Carr, Christopher B. Stell, Jessica A. Loveland, and Dan M. Goebel
Jet Propulsion Laboratory, California Institute of Technology,
4800 Oak Grove Dr. Pasadena, CA, 91109, USA
(818) 393-4382; ryan.w.conversano@jpl.nasa.gov

ABSTRACT

A review of the component-level flight qualification efforts and power processing unit development status of the Ascendant Sub-kW Transcelestial Electric Propulsion System (ASTRAEUS) program is presented. Component-level qualification efforts were undertaken for the system's ultra-compact heaterless LaB_6 hollow cathode and electromagnets, both of which employ designs bespoke to ASTRAEUS, as they represent the highest failure risks for the thruster. Through parallel long-duration wear and ignition tests, the ASTRAEUS cathode demonstrated invariant discharge performance over more than 5000 h of operation at its maximum operating current of 4 A and demonstrated more than 25,000 ignition cycles. The ASTRAEUS electromagnets completed their environmental qualification through a demonstration of more than 1200 deep thermal cycles with no indication of coil degradation (the test articles previously completed qualification-level vibration and shock testing). ASTRAEUS's prototype power processing unit has demonstrated more than 92% total power conversion efficiency and class-leading power density & specific power density of 4.5 W/cm^3 & 1670 W/kg, respectively. The various power converters found in the ASTRAEUS power processing unit are reviewed with a focus on the methods by which such high performance was achieved.

INTRODUCTION

The Jet Propulsion Laboratory's (JPL) Ascendant Sub-kW Transcelestial Electric Propulsion System (ASTRAEUS) program aims provide a low-power, low-cost, in-space propulsion technology to enable high-ΔV interplanetary exploration using SmallSats. ASTRAEUS is a fully integrated electric propulsion system, including a low-power Hall thruster, an ultra-compact power processing unit (PPU), a xenon flow controller (XFC, not including a tank or pressure management assembly [PMA]), and a SmallSat-optimized gimbal. ASTRAEUS targets a TRL-6 classification[1] by mid-2021. ASTRAEUS is based around the MaSMi (Magnetically Shielded Miniature) Hall thruster[1], which has a well-documented development history since its inception in 2011[2–11] and has recently demonstrated class-leading performance[12]. Flight qualification efforts for the thruster are underway for the engineering model (EM) thruster, with the approach and methodology for the qualification campaign described in previous publications[13–17].

ASTRAEUS pairs the MaSMi-EM to a high-efficiency PPU[2] with the highest power density of any electric propulsion system to date. To provide the high voltage needed by the anode in such a compact system, a novel PPU topology is under development, replacing the traditional flyback or full-bridge converter with a flying capacitor multi-level (FCML) converter based around Gallium Nitride (GaN) High Electron Mobility Transistors (HEMTs) in order to achieve improved PPU performance in dramatically reduced mass and volume.

Multilevel switched-capacitor converters, such as the FCML converter, provide numerous benefits for Hall Effect thrusters, in both enabling higher anode voltages and reducing PPU mass and volume. Combined with compact power supplies for the cathode keeper, magnet, and housekeeping supplies, the FCML anode converter enables an extremely small (<2 L), lightweight (<3 kg), and efficiency (>95 %) PPU, which is suitably matched to the MaSMi Hall thruster.

In this paper, we describe both the early phases of component-level flight qualification for the engineering model MaSMi-EM, the thruster component of ASTRAEUS, as well as the current development status of the ASTRAEUS PPU. Section II describes the MaSMi-EM cathode lifetime and ignition cycle qualification efforts, followed by a review of the

[1] U.S. Provisional Patent No. 16/205,048

[2] U.S. Provisional Patent No. 62/892,229

thruster's electromagnet environmental qualification efforts in Section III. In Section IV, technical details of the ASTRAEUS PPU are presented, including performance results from each of the four primary PPU converters (discharge, magnet, keeper, and housekeeping). Concluding remarks are made in Section V.

CATHODE QUALIFICTION

The MaSMi Hall thruster incorporates a center-mounted lanthanum hexaboride (LaB_6) heaterless hollow cathode, called MaSMi's LUC (Low-current Ultra-compact hollow Cathode) a.k.a. the ASTRAEUS EM cathode, designed to provide discharge currents from <1 A to 4 A. The engineering model cathode is a fully welded & brazed design with an outer diameter of less than 1.3-cm-outside diameter and a length of less than 1.9-cm. Details of the cathode design and development can be found in Refs. [11,12]. As part of the ASTRAEUS program, the cathode life and performance requirements include demonstrating a minimum of 5700 hours of operation at its maximum 4 A discharge current (corresponding to 100 kg Xe thruster throughput) and a minimum of 1200 ignitions (800 required + 50% margin) [12–14].

Despite having no flight heritage, heaterless hollow cathodes have been the subject of many research programs in industry, governement, and universities since 1981 [18]. The few orificed heaterless hollow cathodes using LaB_6 emitters described in the open literature have been developed for medium-power Hall thrusters (e.g. 3-5 kW) and have demonstrated to survive >10,000 ignitions [19]. However, the novel compact design of MaSMi's LUC [20] introduces new potential failure mechanisms that must be understood and characterized.

To retire risks associated with MaSMi's LUC, a two-part life evaluation test approach was adopted: a long-duration wear test (LDWT) conducted in parallel with a separate ignition cycle test. A brief description of these tests is provided here, with details on the specific approach and methodology for each of these test campaigns provided in Refs. [13,21]. The long-duration wear test aimed at demonstrating ≥2400 cycles (3x the ASTRAEUS requirement) and ≥5700 h of operation at the maximum system discharge current of 4 A (100% ASTRAEUS cathode life requirement). The cathode ignition cycle test aimed at demonstrating >10,000 ignition cycles.

As of March 16, 2020, the ASTRAEUS EM cathode SN001 has demonstrated 1628 ignitions and completed 5090 h of operation at 4 A of discharge current. There have been 9 ventings of the cathode test facility's vacuum chamber throughout the test due to required building maintenance. Nevertheless, the performance of the cathode has been effectively unchanged throughout the test, with all data falling within expected variation given the vent cycles on the facility. This is shown in Fig. 1, where the discharge voltage, keeper floating potential, and accumulated xenon throughput are plotted against operating time for the duration of the LDWT. The timing of the chamber ventings are also presented. EM cathode SN001 showed constant performance (i.e. discharge voltage) with time during continuous operation, with a voltage variation of <4%.

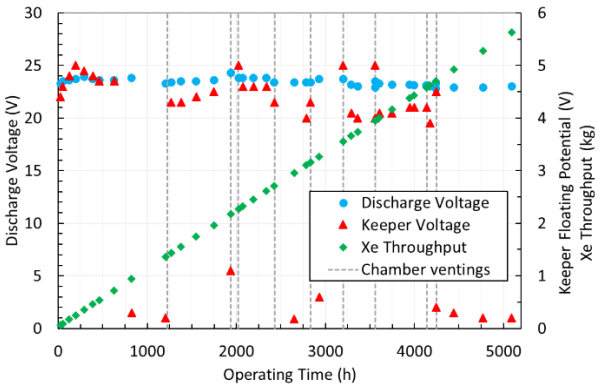

Figure 1. ASTRAEUS cathode discharge voltage, keeper, voltage, and xenon throughput throughout the first ~5000 h of the cathode LDWT. Despite intermittent cathode-to-keeper soft short, cathode discharge performance has remained invariant and cathode retains the ability to be re-ignited.

During the early phases of the cathode LDWT, the test was divided in segments of 220 cathode ignitions followed by 600 h of constant operation at 4 A. Each ignition cycle consisted in three phases: initiate the plasma discharge by applying the required ignition voltage at the keeper with an established propellant flow, maintain the anode discharge for 5s, extinguish the discharge, and finally let the cathode cool for 110s. Cathode performance characterization (discharge/ keeper voltage, plume mode margins, ignition voltage breakdown vs flow) was measured prior to the start of the test and after completion of 4 test segments. The final cathode characterization is pending completion of the planned test segments, which have been delayed due to COVID-19.

After approximately 680 h of operation and <250 ignition cycles, an intermittent keeper-to-cathode short was observed. Each time the short appeared, it was possible to clear it with the application of 150 V and ≤3 A on the keeper without an applied propellant flow (it should be noted that this voltage and current is within the capability of the ASTRAEUS PPU, thereby suggesting such a short could be cleared during space operations).

Cathode discharge performance was not affected by this short during steady state operation, as shown in Fig. 1. Considering the cathode design and nature of the short, it was deduced that the short was likely caused by separation of the heat shield welds, enabling the heat shield (tied to cathode common) to migrate during thermal cycling and contact the keeper. Further evidence of this theory emerged after the cathode ignition cycle testing, as described below.

The dedicated ignition cycle test was performed on ASTRAEUS EM cathode SN002 to determine if tens of thousands of heaterless ignitions were possible, and how such ignitions may affect the normal discharge operation of the cathode. Details of the test approach and results can be found in Ref. [21]; a breif summary is provided herein.

The test was performed in one of the JPL's cathode test facilities that simulates the Hall thruster environment near the cathode plume. The cathode was subjected to repeated "full" ignitions, i.e. striking directly to a 2 A anode discharge, representing a more stressful ignition process than igniting first to a keeper discharge and then to the anode. The duration of each cycle was carefully examinated to guarantee comparable behavior with respect to the nominal cold-start ignition sequence in the least possible time. The first ~18,000 ignition cycles each spanned 8 s: 2 s maintaining an anode discharge and 6 s of cooling time between cycles. The following ~7,000 cycles each spanned 20s: 5 s maintianing an anode discharge and 15 s of cooling time between cycles. This change in cycle timing was performed due to ignition characteristic changes later in the test; however, the cathode never failed to ignite throughout the test. Cathode performance (i.e. anode and keeper voltage at nominal operating conditions) was measured at various times throughout the test to assess repeated ignition effects on steady-state operation. At the end of the test, the cathode was desctructively analyzed.

The cathode demonstrated more than 25,000 heaterless ignitions with no discernable degradation in the steady-state operation performance and no significant damage of the internal surfaces. Slight modifications and morphology changes of several of the cathode surfaces, associated with some microarcing events during the ignition cycles, were observed during post-test analysis but did not affect the cathode performance.

Additional evidence of the aforementioned heat shield migration and contact with the keeper was identified after inspecting the cross-section of ASTRAEUS EM cathode SN002, an image of which appears in Ref. [21]. The heat shield in this cathode appeared to be migrating downstream towards the keeper, though it did not cause a short during the ignition cycle testing. The weld schedule for the heat shield was modified to prevent this issue from appearing in future EM cathodes. No similar shorting issues have been observed with operational testing of updated ASTRAEUS EM cathodes, including the one under test as part of the ongoing MaSMi-EM Hall thruster's long-duration wear test (data to be presented in a future publication).

ELECTROMAGNET QUALIFICTION

Following the cathode, the ASTRAEUS thruster components with the highest identified risk of failure are the electromagnets, specifically the inner magnet coil due to its tighter wire bend radius and higher operating temperature[22]. Therefore, a component-level qualification campaign was carried out on three ASTRAEUS EM inner coil assemblies. The coils were subjected to dynamic (random vibration and shock) environments corresponding to the predicted input loads from the MaSMi-EM structural model, then subjected to thermal vacuum (TVAC) cycle testing. This test approach replicates the sequence of environments that coils in the thruster will experience during launch followed by operation in flight.

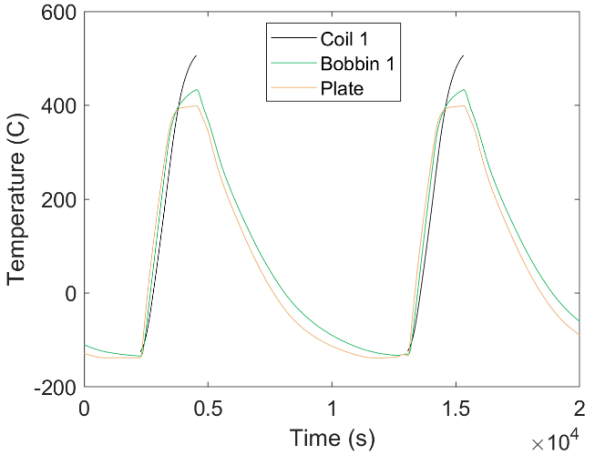

Figure 2. Typical thermal cycle profiles for an ASTRAEUS EM inner electromagnet in the TVAC test. The coil interior temperature (black) could only be determined from the voltage when the coil was powered on, which only occurred during the heating portion of the TVAC cycle.

For TVAC cycling, the coil assemblies were mounted on a copper plate that simulated the thruster's back plate, with an auxiliary heater down the axis of each bobbin. The copper plate was bolted to a stainless steel liquid nitrogen (LN_2)-cooled shroud flange inside a vacuum chamber, with radiation shielding between the coils and the shroud and between the shroud and the chamber wall.

An automated system was used to cycle the coils from -123 +0/-5°C to 500 ±5°C; the coils were unpowered during the cooling portion of each cycle, and during heating they were operated at the maximum magnet current setting. Thermocouples were mounted on the copper plate and spot-welded to the downstream face of each bobbin, while the internal coil temperatures during cycling were calculated from the coil voltages measured by dedicated sense lines, using data from Ref. [23] for the nonlinear temperature dependence of copper's resistivity. Examples of typical thermal cycle profiles during the test are shown in Fig. 2.

The electromagnet qualification requirement was to complete at least 1200 TVAC cycles, 150% of the maximum anticipated number of on/off cycles in flight[24]. Testing was paused roughly every 100 cycles to make room-temperature winding resistance and insulation resistance measurements at the chamber feedthrough. No deterioration in the coil resistance was observed over the course of the test, with the spread in the measurements falling within the range expected from temperature variability within ±2°C. The winding-to-bobbin insulation resistance was measured to be >5 GΩ throughout the test. After completing 1200 cycles, TVAC testing was continued; it is ongoing at the time of writing, with the intention of cycling at least one coil to failure.

POWER PROCESSING UNIT DEVELOPMENT

To accomplish the ASTRAEUS requirements for efficiency, throttleability, and mass [13], a novel PPU is under development, utilizing state of the art converter topologies and GaN semiconductor devices to provide extremely compact and efficient power conversion. The thruster requires three distinct power supplies: a discharge (i.e. anode) supply capable of providing the high voltage needed for high-specific impulse (I_{sp}) thruster operation, a cathode keeper supply to provide the cathode ignition voltage, and a magnet supply to power the thruster's electromagnets. In addition, the PPU must provide power for its own integrated housekeeping and XFC control electronics. To meet these needs, the PPU has been architected as shown in Fig. 3.

The PPU is required to fit within a 2.5 L and 3.33 kg allocation while achieving greater than 92% combined efficiency (i.e. total output power of all converters vs. total input power for all converters) across its full operating range and supporting mission Total Ionizing Dose (TID) up to 100 krad. This section will describe each PPU element in detail, presenting the methodology for development of each conversion stage to meet these lofty requirements, in addition to prototype testing results that demonstrate the design.

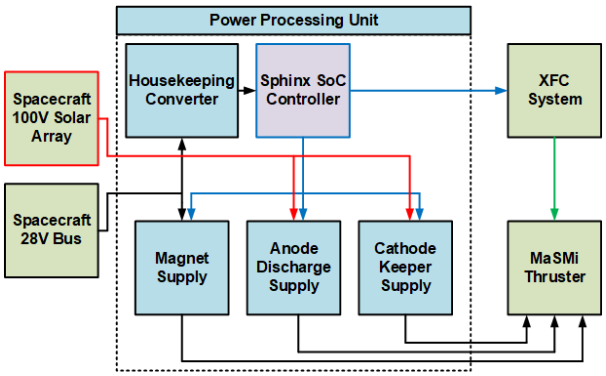

Figure 3. System-level PPU block diagram.

Discharge Supply

The discharge supply generates an electric field between the thruster's anode and cathode which is responsible for accelerating xenon ions to generate thrust. Increased anode voltage in electric thrusters generally correlates to higher system I_{sp}, allowing for reduction in requisite Xenon mass for a given trajectory at the expense complicating anode converter design and reducing PPU efficiency [25,26]. The ASTRAEUS PPU utilizes a FCML boost converter for its discharge supply, providing a distinct advantage over conventional converters in voltage support, throttling capability, and power density.

Firstly, dividing the high voltage output equally over the switching cells in the converter prevents any one switching device from supporting the full output voltage. This enables ASTRAEUS to reach a 500V with low voltage components, rather than relying on diode rectification to achieve high converter performance.

Secondly, most PPU designs opt for a single operating point (or more specifically, a single operating voltage), thereby reducing converter complexity and improving efficiency. The GaN-based FCML utilized in ASTRAEUS enables the converter to provide a fully throttleable output voltage across the range from 200 V – 500 V while also achieving the aforementioned requirements set. Further, the FCML enables the use of GaN HEMTs, which have been shown to be tolerant to both Single Event Effects (SEEs) and TID, making them extremely promising for use in spacecraft power converters [27,28].

Finally, FCML converters require significantly smaller magnetic and capacitive filtering elements when compared with traditional PPU anode supplies [29,30]. This arises from the switching frequency in the inductor being a multiple of the number of converter cells, allowing for improved filtering performance without driving the switching frequencies of the individual cells

higher. As a result, the impedance of the filtering element appears as a multiple of the cell frequency, requiring reduced total capacitance and inductance in the system.

Leveraging the performance benefits inherent to the FCML topology, the discharge supply has been developed to the specifications shown in Table 1. The 6-level FCML that has been designed to these requirements is shown in Fig. 4. Utilizing GS66516T 650V transistors [31], this design limits the applied stress to a single switch to 100 V, well within the derated operating range of 75% that has been demonstrated in SEE testing [27]. Furthermore, it allows individual cells switched at 150 kHz to generate an equivalent inductor current frequency of 900 kHz, reducing the primary inductor volume by 50% over a conventional boost converter. The measured efficiency of the prototype discharge supply, shown in Fig. 5, exceeded 94% across the full 1000 W load range with a peak efficiency of 97.6% at 200 V. The converter is built on a single 11 cm x 10 cm printed circuit board (PCB), achieving power density of 4.5 W/cm^3 (4500 W/L) and specific power of 1670 W/kg. The result is an extremely compact, highly efficient anode converter capable of throttling over the full operating range of the MaSMi Hall thruster.

Table 1: Discharge Supply Specification

Parameter	Minimum	Maximum
Output Power	100 W	1000 W
Input Voltage	26 V	100 V
Output Voltage	200 V	500 V
Output Current	0.5 A	4 A

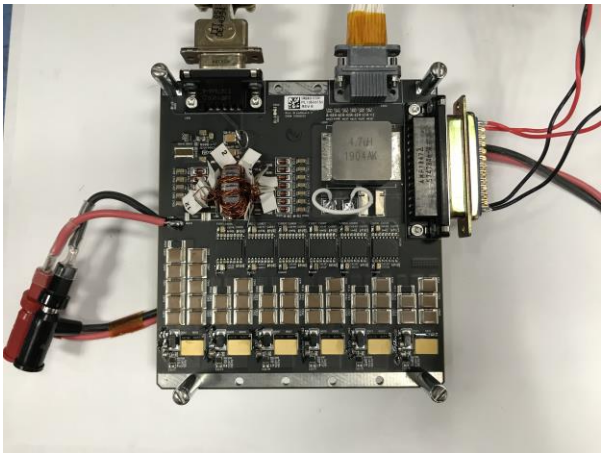

Figure4. Prototype discharge supply.

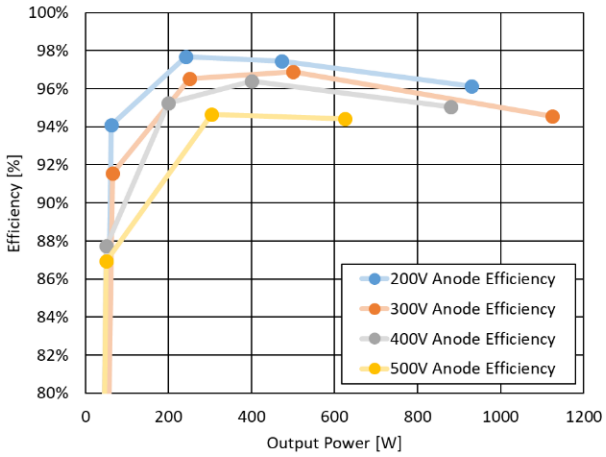

Figure 5. Measured discharge supply efficiency.

Housekeeping Supply

The performance merits of the FCML for high-voltage, high-power, and throttleable anode supplies comes at the cost of the well-demonstrated complexity of designing FCML drive systems. Each gate driver requires an independent power supply referenced to the FET's source, creating a large amount of external circuitry. This has been solved in previous FCML designs via several methods, including bootstrapping diodes [32], individual isolated converters [33], and charge pumps [34]. However, all of these solutions add significant component count to the circuitry for each individual switch, resulting in significantly increased total volume. While not an issue in terrestrial power supplies, the same circuitry in spacecraft FCML designs was found to be prohibitively massive for ASTRAEUS. Instead, a dedicated housekeeping supply has been designed, which utilizes a 13-winding asynchronous flyback converter. The converter provides 5 V rails referenced to each GaN switching stage and provides power to the system on chip (SoC) controller which drives the PPU. The specifications for the housekeeping supply are given in Table 2.

Table 2: Housekeeping Supply Specification

Parameter	Minimum	Maximum
Output Power	0 W	18 W
Input Voltage	22 V	36 V
Output Voltage	0 V	6 V
Output Current	0 A	3 A

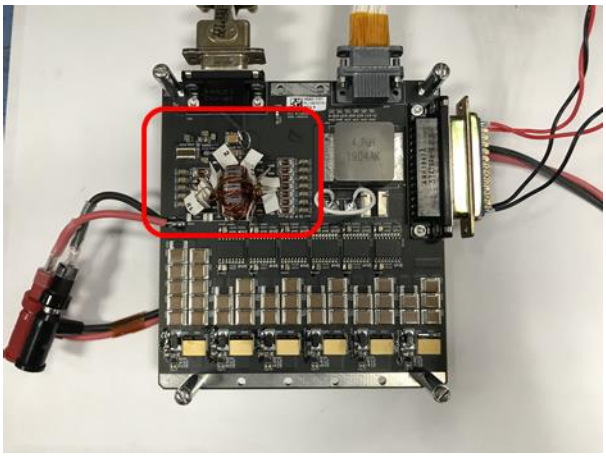

Figure 6. Prototype housekeeping supply.

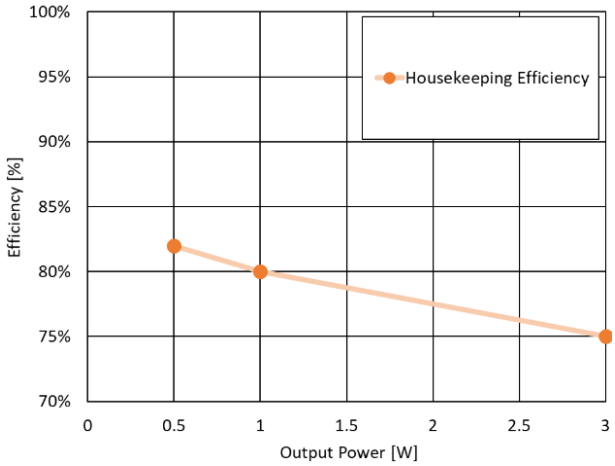

Figure 7. Measured housekeeping supply efficiency.

The multi-output flyback designed to meet these specifications utilizes discontinuous condition mode (DCM) to maximize efficiency with diode rectification. The low currents on the auxiliary windings make DCM with asynchronous rectification a more mass and power efficient solution for spacecraft application, where the terrestrial solutions described previously hare prohibitively volume and mass intensive. The resulting design is co-located on the same PCB as the anode supply, reducing coupled noise injection into the floating gate drive rails and minimizing PCB area for the overall design. The prototype housekeeping supply is highlighted on the discharge supply PCB in Fig. 6; its demonstrated efficiency is presented in Fig. 7. The housekeeping supply achieves full load efficiency of 75%, with a peak efficiency of 85%.

Keeper Supply

The keeper supply must provide high voltage to ignite the cathode as well as provide a steady state current to keep the cathode lit in select low-power operational states. These two needs conflict in converter design, resulting in the specifications shown in Table 3.

Table 3: Keeper Supply Specification

Parameter	Minimum	Maximum
Output Power	0 W	100 W
Input Voltage	22 V	36 V
Output Voltage	0 V	1000 V
Output Current	0.5 A	3 A

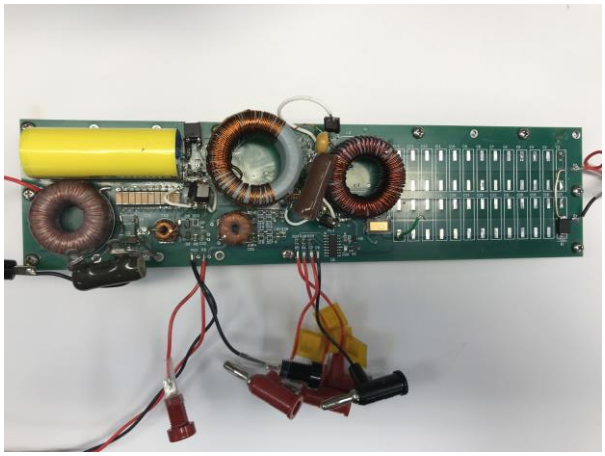

Figure 8. Prototype keeper supply.

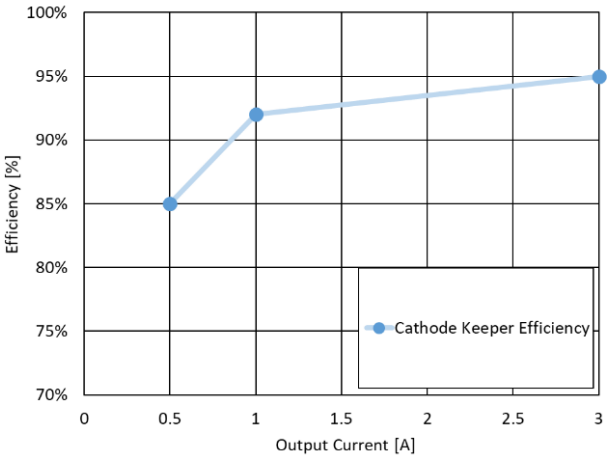

Figure 9. Measured keeper supply efficiency.

To develop a converter which provides both high output voltage and efficient low voltage conversion for a steady state current, a two-switch forward converter in a boost configuration was developed. Utilizing a 20 kHz Si MOSFET design, high conversion ratio and efficiency can be maintained, while minimizing oscillation during

the ignition transient. The resulting prototype is shown in Fig. 8 with its efficiency presented in Fig. 9; 95% efficiency was demonstrated at the full 3 A output.

Magnet Supply

To power the thruster's electromagnets, a current-controlled magnet supply has been developed. The specifications for this supply are given in Table 4.

Table 4: Magnet Supply Specification

Parameter	Minimum	Maximum
Output Power	0 W	120 W
Input Voltage	22 V	36 V
Output Voltage	0 V	30 V
Output Current	0 A	4 A

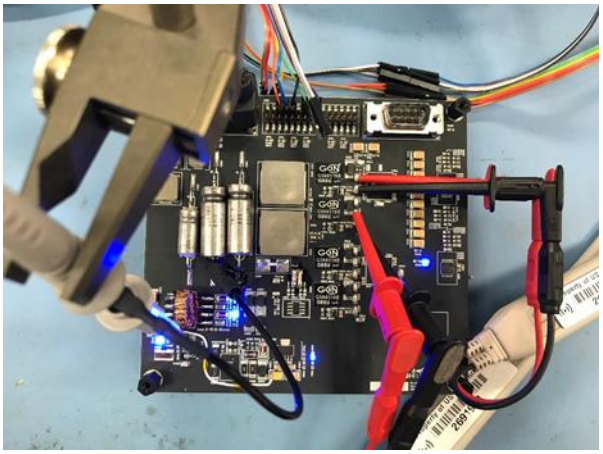

Figure 10. Prototype magnet supply.

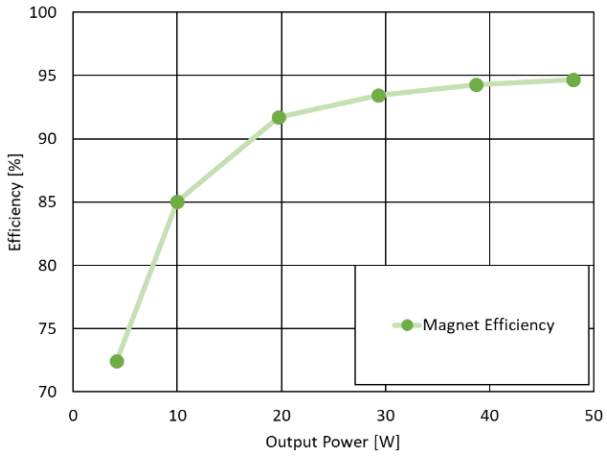

Figure 11. Measured magnet supply efficiency

Due to the overlap of the input and output voltage ranges, a four-switch, noninverting, buck-boost converter has been developed utilizing GS61008T FETs to achieve efficient conversion at ranges up to 1 MHz [35]. The converter utilizes a new hysteretic control algorithm to manage magnet current. The designed prototype, shown in Fig. 10, operates at 150 kHz to optimize for efficiency, as shown in Fig. 11. The converter achieves full load efficiency of 95% at the full load 4 A output.

CONCLUSION

A review of the ASTRAEUS thruster's component-level flight qualification efforts and power processing unit's development was presented. The MaSMi thruster's novel hollow cathode has successfully completed more than 5000 h of a long-duration wear test targeting >10,000 h of operation with no change in its discharge performance. The cause for the observed intermittent short between the keeper and cathode was identified, and clearing the short with an energy pulse within the capability of the ASTRAEUS power processing unit was demonstrated. The fundamental cause for the short was addressed, and subsequent cathode builds have not exhibited the same issue. The ASTRAEUS cathode also successfully demonstrated more than 25,000 ignition cycles directly to an anode discharge, never failing to ignite throughout the test. Having previously completed a dynamic (random vibration and shock) test campaign, a set of ASTRAEUS's unique electromagnets were subjected to a thermal vacuum cycling campaign. The coils successfully completed more than 1200 deep thermal cycles with no indication of degradation. The prototype ASTRAEUS power processing unit was shown to operate at more than 92% total conversion efficiency across its entire operating range. The topology, fundamentals of operation, and performance of each of the four power converters found in the power processing unit were discussed. In summary, the power processing unit demonstrated class-leading power density and specific power density, which were natural results of meeting the challenging ASTRAEUS requirements.

ACKNOWLEDGEMENTS

The authors would like to acknowledge the programmatic support and contributions provided by Satish Khanna (JPL), John Baker (JPL), and Ron Reeve (JPL). This research was carried out at the Jet Propulsion Laboratory, California Institute of Technology, under a contract with the National Aeronautics and Space Administration and funded through the internal Research and Technology Development program.

REFERENCES

[1] Frerking, M. A. and Beauchamp, P. M., "JPL Technology Readiness Assessment Guideline," *2016 IEEE Aerospace Conference*, Big Sky, MT, Mar. 2016.

[2] Conversano, R. W., Goebel, D. M., Hofer, R. R., Matlock, T. S., and Wirz, R. E., "Development and Initial Testing of a Magnetically Shielded Miniature Hall Thruster," *IEEE Trans. Plasma Sci.*, vol. 43, no. 1 (2015).

[3] Conversano, R. W., Arora, N., Goebel, D. M., and Wirz, R. E., "Preliminary Mission Capabilities Assessment of a Magnetically Shielded Miniature Hall Thruster," IAC-14.C4.4.4, *65th IAF/IAA/IISL International Astronaturical Congress*, Toronto, Canada, Oct. 2014.

[4] Conversano, R. W., Goebel, D. M., Mikellides, I. G., Hofer, R. R., Matlock, T. S., and Wirz, R. E., "Magnetically Shielded Miniature Hall Thruster: Performance Assessment and Status Update," AIAA-2014-3896, *50th AIAA Joint Propulsion Conference*, Cleveland, OH, Jul. 2014.

[5] Conversano, R. W., Goebel, D. M., Hofer, R. R., Mikellides, I. G., Katz, I., and Wirz, R. E., "Magnetically Shielded Miniature Hall Thruster: Design Improvement and Performance Analysis," IEPC-2015-100 / ISTS-2015-b-100, *34th ERPS International Electric Propulsion Conference*, Kobe, Japan, Jul. 2015.

[6] Conversano, R. W., "Low-Power Magnetically Shielded Hall Thrusters," Ph.D. Thesis, Department of Mechanical and Aerospace Engineering, University of California, Los Angeles, 2015.

[7] Conversano, R. W., Arora, N., Strange, N. J., and Goebel, D. M., "An Enabling Low-Power Magnetically Shielded Hall Thruster for Interplanetary Smallsat Missions," *Interplanetary Small Satellite Conference*, Pasadena, CA, Apr. 2016.

[8] Conversano, R. W., Goebel, D. M., Hofer, R. R., and Arora, N., "Performance enhancement of a long-life, low-power hall thruster for deep-space smallsats," *IEEE Aerospace Conference*, Big Sky, MT, Mar. 2017.

[9] Conversano, R. W., Goebel, D. M., Hofer, R. R., Mikellides, I. G., and Wirz, R. E., "Performance analysis of a low-power magnetically shielded hall thruster: Experiments," *J. Propuls. Power*, vol. 33, no. 4 (2017).

[10] Conversano, R. W., Goebel, D. M., Mikellides, I. G., Hofer, R. R., and Wirz, R. E., "Performance analysis of a low-power magnetically shielded hall thruster: Computational modeling," *J. Propuls. Power*, vol. 33, no. 4 (2017).

[11] Conversano, R. W., Lobbia, R. B., Tilley, K. C., Goebel, D. M., Reilly, S. W., Mikellides, I. G., and Hofer, R. R., "Development and Initial Performance Testing of a Low-Power Magnetically Shielded Hall Thruster with an Internally-Mounted Hollow Cathode," IEPC-2017-64, *35th International Electric Propulsion Conference*, Atlanta, GA, Oct. 2017.

[12] Conversano, R. W., Lobbia, R. B., Kerber, T. V., Tilley, K. C., Goebel, D. M., Reilly, S. W., Mikellides, I. G., and Hofer, R. R., "Performance Characterization of a Low-Power Magnetically Shielded Hall Thruster with an Internally-Mounted Hollow Cathode," *Plasma Sources Sci. Technol.*, (2019).

[13] Conversano, R. W., Barchowsky, A., Lobbia, R. B., Chaplin, V. H., Lopez Ortega, A., Loveland, J. A., Lui, A. D., Becatti, G., Reilly, S. W., Goebel, D. M., Snyder, J. S., Hofer, R. R., Randolph, T. M., Mikellides, I. G., Vorperian, V., Carr, G. A., Rapinchuk, J., Villalpando, C. Y., and Grebow, D., "Overview of the Ascendant Sub-kW Transcelestial Electric Propulsion System (ASTRAEUS)," IEPC-2019-282, *36th International Electric Propulsion Conference*, Vienna, Austria, Sep. 2019.

[14] Conversano, R. W., Reilly, S. W., Kerber, T. V., Brooks, J. W., and Goebel, D. M., "Development of and Acceptance Test Preparations for the Thruster Component of the Ascendant Sub-kW Transcelestial Electric Propulsion System (ASTRAEUS)," IEPC-2019-283, *36th International Electric Propulsion Conference*, Vienna, Austria, Sep. 2019.

[15] Lobbia, R., Conversano, R., Lopez Ortega, A., Reilly, S., and Mikellides, I., "Pole Erosion Measurements for the Development Model of the Magnetically Shielded Miniature Hall Thruster (MaSMi-DM)," IEPC-2019-298, *36th International Electric Propulsion Conference*, Vienna, Austria, Sep. 2019.

[16] Chaplin, V. H., Conversano, R. W., Lopez Ortega, A., Mikellides, I. G., Lobbia, R. B., and Hofer, R. R., "Ion Velocity Measurements in the Magnetically Shielded Miniature Hall Thruster (MaSMi) Using Laser-Induced Fluorescence," IEPC-2019-531, *36th International Electric Propulsion Conference*, Vienna, Austria, Sep. 2019.

[17] Lopez Ortega, A., Mikellides, I. G., Conversano, R. W., Lobbia, R. B., and Chaplin, V. H., "Plasma Simulations for the Assessment of Pole Erosion in the Magnetically Shielded Miniature

(MaSMi) Hall Thruster," IEPC-2019-281, *36th International Electric Propulsion Conference*, Vienna, Austria, Sep. 2019.

[18] Lev, D. R., Mikellides, I. G., Pedrini, D., Goebel, D. M., Jorns, B. A., and Mcdonald, M. S., "Recent progress in research and development of hollow cathodes for electric propulsion," *Rev. Mod. Plasma Phys.*, vol. 3, no. 6 (2019).

[19] Ning, Z.-X., Zhang, H.-G., Zhu, X.-M., Ouyang, L., Liu, X.-Y., Jiang, B.-H., and Yu, D.-R., "10000-Ignition-Cycle Investigation of a LaB6 Hollow Cathode for 3–5-Kilowatt Hall Thruster," *J. Propuls. Power*, (2018).

[20] Conversano, R. W., Goebel, D. M., Katz, I., and Hofer, R. R., "Low-Power Hall Thrsuter with an Internally Mounted Low-Current Hollow Cathode," US Patent No. 16/205,0482019.

[21] Becatti, G., Conversano, R. W., and Goebel, D. M., "Demonstration of 25,000 Ignitions on a Proto-Flight Compact Heaterless LaB6 Hollow Cathode," *Plasma Sources Sci. Technol.*, vol. Submitted, (2020).

[22] Myers, J., Kamhawi, H., Yim, J. T., and Clayman, L., "Hall Thruster Thermal Modeling and Test Data Correlation," AIAA-2016-4535, *52nd AIAA/SAE/ASEE Joint Propulsion Conference*, Salt Lake City, UT, Jul. 2016.

[23] Matula, R. A., "Electrical resistivity of copper, gold, palladium, and silver," *J. Phys. Chem. Ref. Data*, vol. 8, no. 4, pp. 1147–1298 (1979).

[24] Polk, J. E. and Brophy, J. R., "Life Qualification of Hall Thrusters By Analysis and Test," 00547, *Space Propulsion 2018*, Seville, Spain, May 2018.

[25] Hofer, R., "High-Specific Impulse Operation of the BPT-4000 Hall Thruster for NASA Science Missions," AIAA-2010-6623, *46th AIAA/ASME/SAE/ASEE Joint Propulsion Conference*, Nashville, TN, Jul. 2010.

[26] Chen, Y., Bradley, T., Iannello, C. J., Carr, G. A., Mojarradi, M. M., Hunter, D. J., Del Castillo, L., and Stell, C. B., "High Temperature Boost (HTB) Power Processing Unit (PPU) Formulatoin Study," *NASA*, (2013).

[27] Scheick, L., "Single-event Effect Report for EPC Series eGaN FETs : Comparison of EPC1000 and EPC2000 series devices for destructive SEE," Pasadena, CA, (2014).

[28] Scheick, L., "Status of the Wide Bandgap Working Group," *NASA Electronic Parts and Packaging (NEPP) Program Electronic Technology Workgroup*, 2016.

[29] Barchowsky, A., Kozak, J. P., Grainger, B. M., Stanchina, W. E., and Reed, G. F., "A GaN-Based Modular Multilevel DC-DC Converter for High-Density Anode Discharge Power Modules," *IEEE Aerospace Conference*, Big Sky, MT, 2017.

[30] Rentmeister, J. S., Schaef, C., Foo, B. X., and Stauth, J. T., "A Flying Capacitor Multilevel Converter with Sampled Valley-Current Detection for Multi-Mode Operation and Capacitor Voltage Balancing," *IEEE Energy Conversion Congress and Exposition*, Milwaukee, WI, 2016.

[31] GaN Systems, "GS66516T, Top-side cooled 650 V E-mode GaN transistor, Datasheet (rev. 200402)," 2020. .

[32] Ye, Z., Lei, Y., Lui, W.-C., Shenoy, P. S., and Pilawa-Podgurski, R. C. N., "Improved Bootstrap Methods for Powering Floating Gate Drivers of Flying Capacitor Multilevel Converters and Hybrid Switched-Capacitor Converters," *IEEE Trans. Power Electron.*, vol. 35, no. 6, pp. 5965–5977 (2020).

[33] Analog Devices, "ADuM5210 Datasheet," 2020. .

[34] Ye, Z., Lei, Y., Lui, W.-C., Shenoy, P. S., and Pilawa-Podgurski, R. C. N., "Design and Implementation of a Low-cost and Compact Floating Gate Drive Power Circuit for GaN-based Flying Capacitor Multi-Level Converters," *IEEE Applied Power Electronics Conference and Exposition*, Tampa, FL, Mar. 2017.

[35] GaN Systems, "GS61008T, Top-side cooled 100 V E-mode GaN transistor, Datasheet (rev. 200402)," 2020. .